

# Articles

## FT-IR Study of the Gas-Phase Autoxidation of Trimethylgermane

Philip G. Harrison\* and David M. Podesta

Department of Chemistry, University of Nottingham, University Park,  
Nottingham NG7 2RD, U.K.

Received November 5, 1993\*

The kinetics and mechanism of the autoxidation of trimethylgermane in the gas phase has been investigated in the temperature range 493–533 K using Fourier transform infrared spectroscopy. Over a wide molar ratio of reactants ( $\text{Me}_3\text{GeH}:\text{O}_2$  ratio in the range (1:1)–(1:31)) the loss of  $\text{Me}_3\text{GeH}$  follows second-order kinetics but is independent of oxygen abundance. The products of the reaction are hexamethyldigermoxane,  $\text{Me}_3\text{GeOGeMe}_3$ , and water. No other products are apparent. For a 1:10  $\text{Me}_3\text{GeH}:\text{O}_2$  molar ratio, second-order rate constants vary from  $2.46 \text{ mol}^{-1} \text{ dm}^3 \text{ s}^{-1}$  at 493 K to  $64.1 \text{ mol}^{-1} \text{ dm}^3 \text{ s}^{-1}$  at 533 K. The activation energy for the process is determined to be  $190 \pm 19 \text{ kJ mol}^{-1}$ . The proposed mechanism involves an initial abstraction of the hydridic hydrogen atom from germanium followed by the reaction of the trimethylgermyl radical thus formed with oxygen, giving the (trimethylgermyl)peroxyl radical. This radical is converted into trimethylgermyl hydroperoxide,  $\text{Me}_3\text{GeOOH}$ , by further H-abstraction from  $\text{Me}_3\text{GeH}$  and undergoes O–O bond fission to form (trimethylgermyl)oxyl and hydroxyl radicals. The radicals thus produced propagate the reaction by H-abstraction from  $\text{Me}_3\text{GeH}$ , forming the intermediate  $\text{Me}_3\text{GeOH}$  and water. Hexamethyldigermoxane is subsequently formed by self-condensation of two  $\text{Me}_3\text{GeOH}$  molecules.

### Introduction

Organogermanium hydrides,  $\text{R}_n\text{GeH}_{4-n}$  ( $n = 1-3$ ), are known to undergo slow oxidation in the liquid or solution phases on exposure to air to afford the corresponding organogermanium oxides or hydroxides.<sup>1</sup> Although the susceptibility toward aerial oxidation generally increases as the value of  $n$  decreases, little is known concerning the kinetics or mechanisms of such autoxidation reactions. The gas-phase autoxidation of monogermene in a static system has been examined in some detail.<sup>2</sup> No hydrogen or volatile germanium compounds were formed, and the only germanium-containing product is a white solid, presumed to be  $\text{GeO}_2$  or  $\text{Ge}(\text{OH})_2$ . This solid product was observed to catalyze further reaction, and the kinetics under these conditions were zero order in oxygen and second order in germane at 433–453 K with an activation energy of approximately  $100 \text{ kJ mol}^{-1}$ . The interpretation of these data was qualitative in terms of a radical chain mechanism with a significant surface contribution. The autoxidation of bis(trimethylgermyl)mercury in *n*-octane solution is also zero order in oxygen but, in contrast, first order in the germerylmercurial. From the lack of inhibition by radical traps such as galvinoxyl, the reaction was deduced to follow a molecular pathway involving the formation and subsequent decomposition of germerylperoxide intermediates.<sup>3</sup> In a previous study we have shown

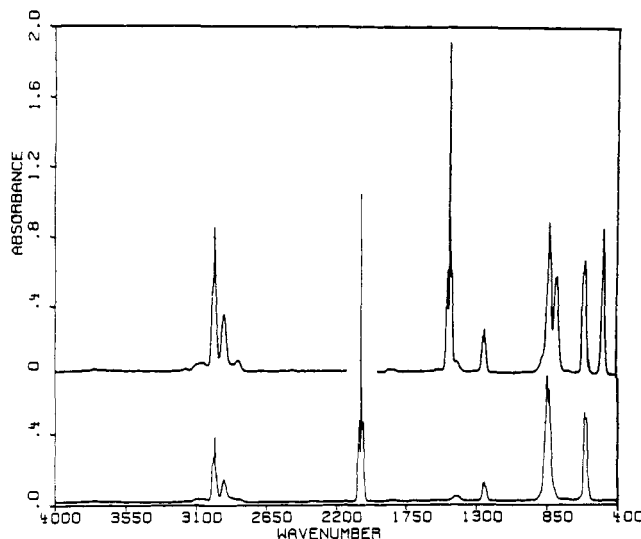
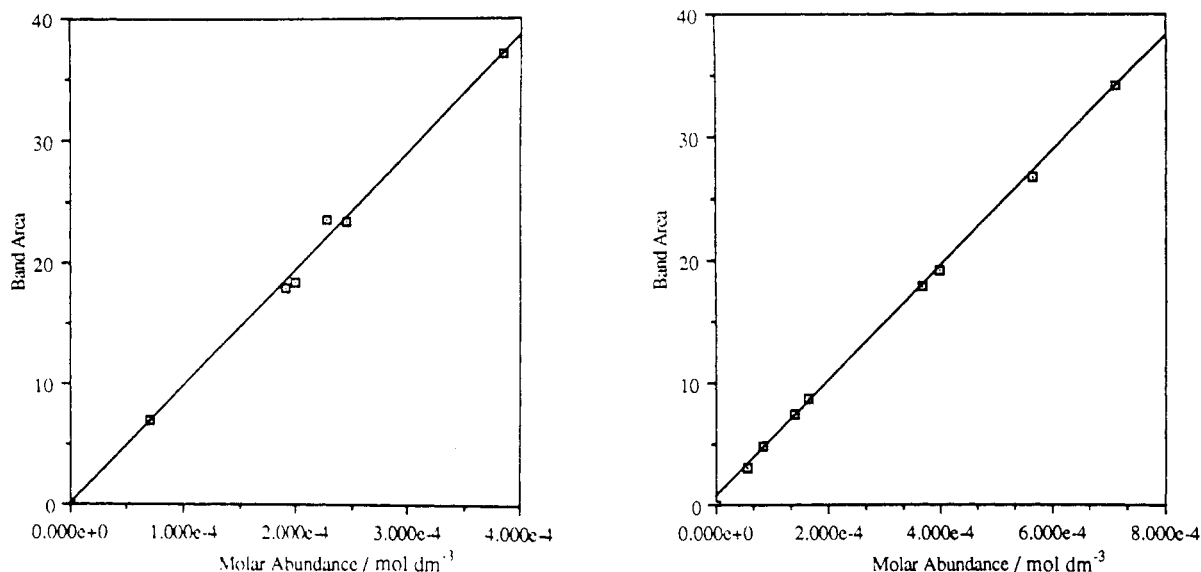


Figure 1. Ambient-temperature gas-phase FT-IR spectra in the range 4000–400  $\text{cm}^{-1}$  for  $\text{Me}_3\text{GeH}$  (lower, 4.7 Torr) and  $\text{Me}_3\text{GeD}$  (upper, 10.5 Torr).

that the thermolysis of neat trimethylgermane in the gas phase in the temperature range 673–873 K follows half-order kinetics with an activation energy of  $260 \text{ kJ mol}^{-1}$ , interpreted by us in terms of a free-radical chain process.<sup>4</sup> In this paper we report a detailed study of the gas-phase autoxidation of trimethylgermane in order to ascertain the mechanistic character of this reaction.

\* Abstract published in *Advance ACS Abstracts*, March 15, 1994.  
(1) Glockling, F. *The Chemistry of Germanium*; Academic Press: London, 1969; p 87.  
(2) Emeleus, H. J.; Gardner, E. R. *J. Chem. Phys.* 1938, 1900.  
(3) Razuvaev, G. A.; Aleksandrov, Y. A.; Glushakova, V. N.; Figurova, G. N. *J. Organomet. Chem.* 1969, 14, 349.

(4) Harrison, P. G.; McManus, J.; Podesta, D. M. *J. Chem. Soc., Chem. Commun.* 1992, 291.



**Figure 2.** Beer plots of  $\text{Me}_3\text{GeH}$  (left, slope  $9.64 \text{ au cm}^{-1} \text{ Torr}^{-1}$ ) and  $\text{Me}_3\text{GeD}$  (right, slope  $4.70 \text{ au cm}^{-1} \text{ Torr}^{-1}$ ).

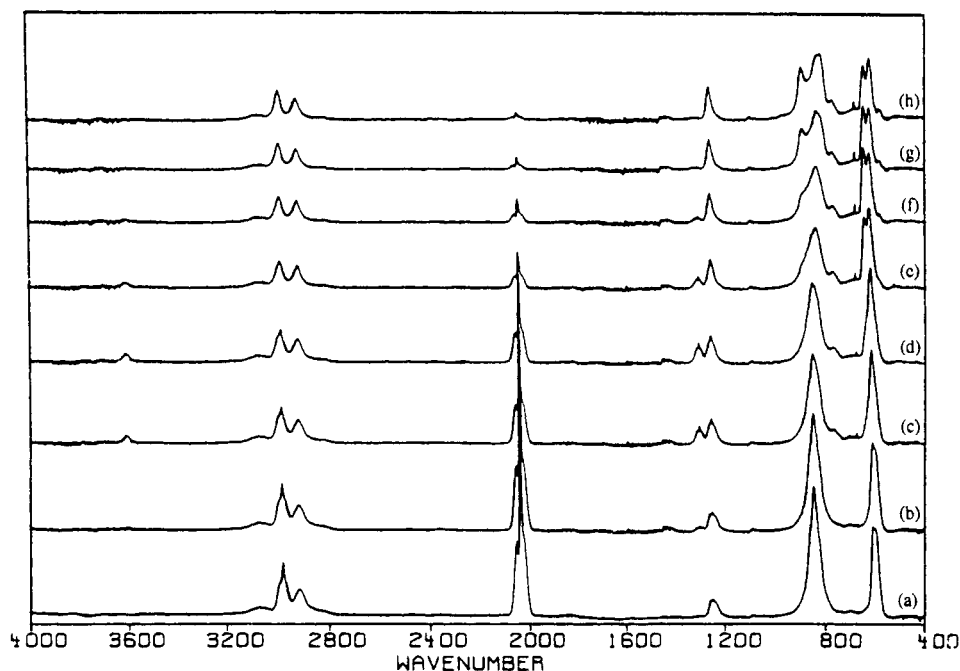


**Figure 3.** FT-IR spectra in the range  $4000\text{--}400 \text{ cm}^{-1}$  for the reaction of a 1:10 mole ratio mixture of  $\text{Me}_3\text{GeH}$  and  $\text{O}_2$  at 493 K (a), at 513 K (b), and at 513 K after 260 s (c), 370 s (d), 915 s (e), 1388 s (f), 2560 s (g), and 3600 s (h) after the start of the experiment.

### Experimental Section

Trimethylgermane was prepared<sup>5</sup> by the reduction of  $\text{Me}_3\text{GeCl}$  (Aldrich Chemical Co. Ltd.) using  $\text{LiAlH}_4$  (95+%, Aldrich Chemical Co. Ltd.) in triethylene glycol dimethyl ether solvent under argon.  $\text{LiAlD}_4$  (98% D, Aldrich Chemical Co. Ltd.) was used for the preparation of trimethylgermane-*d*. The hydride was transferred to a conventional Schlenk line, on which all subsequent manipulations were carried out. For experiments involving neat hydride, a known pressure of hydride was admitted to the infrared cell at ambient temperature. The hydride/oxygen mixtures were prepared using a gas bulb fitted with a small reservoir. A known pressure of the hydride was allowed into the bulb, which was then sealed. The hydride was then isolated in the reservoir by freezing with liquid nitrogen. The desired pressure of oxygen (99.99%, BDH Chemicals Ltd.) was admitted

into the remainder of the bulb prior to opening the reservoir and allowing the two components to mix.

The decomposition of 1:10 trimethylgermane/ $\text{O}_2$  mixtures was studied over the temperature range 453–533 K using approximately 100 Torr pressure of the mixture for each kinetic run. The dependence of the reaction rate on the oxygen abundance was investigated by monitoring the decomposition of the trimethylgermane/ $\text{O}_2$  mixtures for mole ratios ranging from 1:1 to 1:31, all at 493 K. In these experiments the pressure of the mixture admitted into the cell was varied in order to maintain the same abundance of trimethylgermane for each of the mixtures.

To investigate the effect of available surface area on the decomposition, experiments were carried out with known amounts of ground Pyrex glass being added to the cell. After each aliquot had been added, the cell was reconditioned by three separate decompositions of the trimethylgermane/ $\text{O}_2$  mixtures at 533 K prior to the kinetic run being carried out at 493 K.

(5) Wilkinson, G., Stone, F. G. A., Abel, E. W., Eds. *Comprehensive Organometallic Chemistry*; Pergamon Press: Oxford, U.K., 1982; Vol. 2.

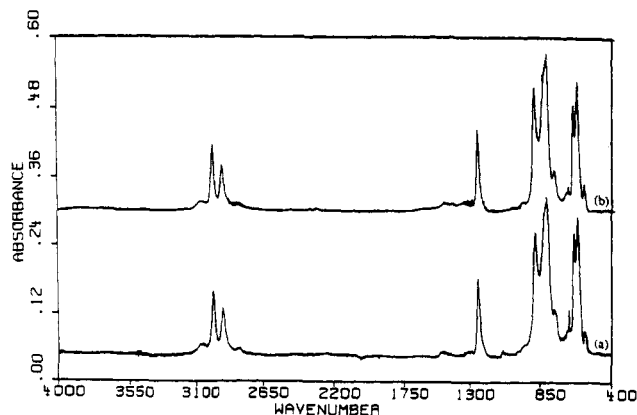


**Figure 4.** Gas-phase FT-IR spectra recorded at ambient temperature of the products obtained after reaction of  $\text{Me}_3\text{-GeH}/\text{O}_2$  (a) and  $\text{Me}_3\text{-GeD}/\text{O}_2$  (b) mixtures.

All infrared measurements were carried out using a Nicolet 20SXC spectrometer. Mass spectra were recorded using a Micromass VG 7070E mass spectrometer.

### Results

Ambient-temperature gas-phase infrared spectra for trimethylgermane and trimethylgermane-*d* are shown in Figure 1. Band positions for both molecules agree with those reported previously<sup>6,7</sup> ( $\nu(\text{Ge-H})$  2040 vs  $\text{cm}^{-1}$ ,  $\nu(\text{Ge-D})$  1470 vs  $\text{cm}^{-1}$ ). Beer plots are shown in Figure 2.

**Identification of Reaction Products.** Figure 3 shows the changes observed in the infrared spectra recorded throughout the course of the reaction of the 1:10 trimethylgermane/ $\text{O}_2$  mixture at 513 K, at which temperature the reaction is virtually complete after 1 h. Clearly evident is the diminution of the  $\nu(\text{Ge-H})$  *P,Q,R*-structured envelope centered at 2040  $\text{cm}^{-1}$ . New bands due to product formation are particularly visible below 1400  $\text{cm}^{-1}$ , and the presence of an intermediate with bands at 3606 and 1295  $\text{cm}^{-1}$  is observed after *ca.* 500 s into the reaction. Methane, methanol, carbon monoxide, and carbon dioxide are totally absent. The ultimate germanium-containing product of the reaction is hexamethyldigermoxane, which is formed from both  $\text{Me}_3\text{-GeH}/\text{O}_2$  and  $\text{Me}_3\text{-GeD}/\text{O}_2$  mixtures (Figure 4) and was identified unequivocally by a combination of infrared (Table 1),  $^1\text{H}$  NMR and mass spectral data. No other germanium-containing product is apparent.

The mass spectrum of the products obtained after reaction of the  $\text{Me}_3\text{-GeH}/\text{O}_2$  mixture is shown in Figure 5. The fragment of highest *m/e* value is observed as a polyisotopic fragment ranging from *m/e* 231 to 245 with maximum intensity at *m/e* 237. This fragment exhibits the isotopic distribution pattern characteristic of a species containing two germanium atom,<sup>8</sup> and the *m/e* value corresponds to the  $[\text{Me}_3\text{Ge}_2\text{O}]^+$  ion. Other monogermanium-containing fragments which are clearly discernible and which also arise from  $\text{Me}_3\text{GeOGeMe}_3$  occur at *m/e ca.* 119 ( $[\text{Me}_3\text{Ge}]^+$  and  $\{\text{Me}_2\text{GeO}\}^+$ ), *m/e ca.* 105 ( $[\text{Me}_2\text{Ge}]^+$  and  $[\text{MeGeO}]^+$ ), and *m/e ca.* 89 ( $[\text{MeGe}]^+$  and  $\{\text{GeOH}\}^+$ ). A  $\text{CCl}_4$  solution of the product recovered from a typical reaction exhibited a single resonance at  $\delta$  0.29 ppm (*cf.* 0.29<sup>9</sup> and 0.31<sup>10</sup> for hexamethyldigermoxane).

**Table 1.** Infrared Data ( $\text{cm}^{-1}$ ) for Reaction Products and for Hexamethyldigermoxane

reacn product	$\text{Me}_3\text{GeOGeMe}_3$		assignt
	soln <sup>a</sup>	pure liquid <sup>b</sup>	
2984 s	2983 vs		$\nu_a, \nu_s(\text{C-H})$
2918 s	2914 vs		$\nu_s(\text{C-H})$
2808 w	2793 vw		
1435 w, sh	1433 w		$\delta_a(\text{CH}_3)$
1410 m	1408 w	1408	$\delta_a(\text{CH}_3)$
1340 m	1330 w	1332 vw	$\delta_a(\text{CH}_3)$
1245 s	1236 vs	1236 m	$\delta_s(\text{CH}_3)$
952 m	966 sh		
882 vs	859 s	870 s	$\rho(\text{CH}_3)$ and $\nu_s(\text{GeOGe})$
814 vs, sh	823 vs	822 s	$\rho(\text{CH}_3)$ and $\nu_s(\text{GeOGe})$
802	794 vs	796 vs	$\rho(\text{CH}_3)$ and $\nu_s(\text{GeOGe})$
757 s	753 s	755 m	$\rho(\text{CH}_3)$ and $\nu_s(\text{GeOGe})$
669 m	653 w		
609 s	607 s	612 m	$\nu_s(\text{GeC}_3)$
567 m	566 m	570 m	$\nu_s(\text{GeC}_3)$

<sup>a</sup> Marchand, A.; Forel, M. T.; Lebedeff, M.; Valade, J. *J. Organomet. Chem.* **1971**, *26*, 69. <sup>b</sup> Brown, M. P.; Okawara, R.; Rochow, E. G. *Spectrochim. Acta* **1960**, *16*, 595.

The intermediate which is formed during the course of the reactions is characterized by bands at 3606 and 1295  $\text{cm}^{-1}$  (Figure 6) which are shifted to 2660 and 975  $\text{cm}^{-1}$ , respectively, when  $\text{Me}_3\text{-GeD}$  is employed and may be assigned as the  $\nu(\text{O-H/D})$  and  $\delta(\text{O-H/D})$  signals<sup>11,12</sup> of either the germanol  $\text{Me}_3\text{-GeOH}$  or the germyl hydroperoxide  $\text{Me}_3\text{-GeOOH}$ . In view of the thermal instability of the latter, we prefer the former. Indeed, germanols are known intermediates during the formation of digermoxanes from chlorotriorganogermanes.<sup>13,14</sup> The other product observed is  $\text{H}_2\text{O}/\text{D}_2\text{O}$  (Figure 7).

**Reaction Kinetics.** The progress of the autoxidation of  $\text{Me}_3\text{-GeH}$  was monitored by measuring the decrease in the area of the band envelope of the  $\nu(\text{Ge-H})$  stretching mode (Figure 8) which can be converted into molar gas-phase abundance using the Beer law data. The order of the reaction with respect to loss of  $\text{Me}_3\text{-GeH}$  was determined to be 2 from van't Hoff plots (Figure 9), and second-order rate plots for the loss of  $\text{Me}_3\text{-GeH}$  over the temperature range 493–533 K are shown in Figure 10. Numerical rate constant data are collected in Table 2. Below 493 K the reaction is extremely slow, precluding a sufficient extent of reaction to be studied.

The Arrhenius plot over the temperature range studied is shown in Figure 11. The least-squares fit is given by the relationship

$$\ln(k \text{ (mol}^{-1} \text{ dm}^3 \text{ s}^{-1}\text{)}) = (47.2 \pm 4.5) - (190 \pm 19)/RT$$

giving a value of  $190 \pm 19 \text{ kJ mol}^{-1}$  for the activation energy of the reaction.

The effect of changing the oxygen abundance was investigated by measuring the rate of reaction using  $\text{Me}_3\text{-GeH}/\text{O}_2$  mixtures ranging from 1:1 to 1:31. The second-order rate constants obtained for the decomposition of  $\text{Me}_3\text{-GeH}$  at 493 K for each of the mixtures are listed in Table 3 and are essentially constant with a mean value of  $1.9(3) \text{ mol}^{-1} \text{ dm}^3 \text{ s}^{-1}$ . Thus, the reaction is independent of the oxygen abundance over the range studied and, hence, zero order with respect to oxygen.

Decomposition of  $\text{Me}_3\text{-GeH}/\text{O}_2$  mixtures in a pristine glass cell was significantly slower, requiring temperatures

(6) Van de Vondel, G. F.; Van der Kelen, G. P. *Bull. Soc. Chim. Belg.* **1965**, *74*, 467.

(7) Imai, Y.; Aida, K. *Bull. Chem. Soc. Jpn.* **1981**, *54*, 3323.

(8) Glockling, F.; Light, J. R. *J. Chem. Soc. A* **1968**, 717.

(9) Drake, J. E.; Glavinovski, B. M.; Henderson, H. E. *Can. J. Chem.* **1978**, *56*, 465.

(10) Schmidbaur, H.; Ruidisich, I. *Inorg. Chem.* **1964**, *3*, 599.

(11) Matwiyoff, N. A.; Drago, R. S. *J. Organomet. Chem.* **1965**, *3*, 393.

(12) Williams, D. H.; Fleming, I. *Spectroscopic Methods in Organic Chemistry*, 3rd ed.; McGraw Hill: London, 1980; Chapter 3, p 40.

(13) Anderson, H. H. *J. Am. Chem. Soc.* **1953**, *75*, 814.

(14) Brook, A. G.; Gilman, H. *J. Am. Chem. Soc.* **1954**, *76*, 77.

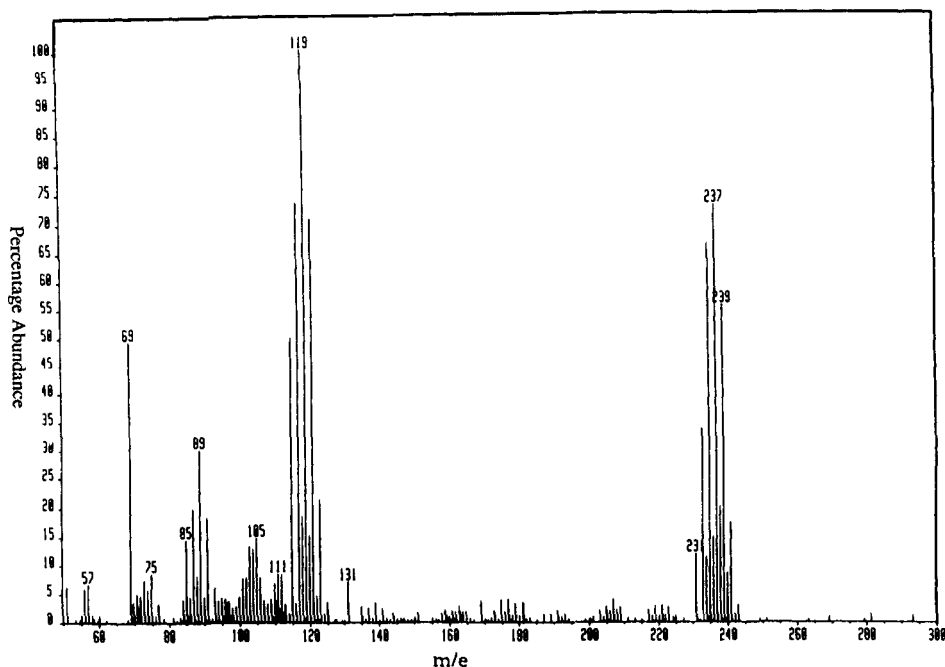


**Figure 5.** Mass spectrum (70 eV) recorded at ambient temperature of the products obtained after reaction of  $\text{Me}_3\text{GeH}/\text{O}_2$  (1:10) at 513 K.

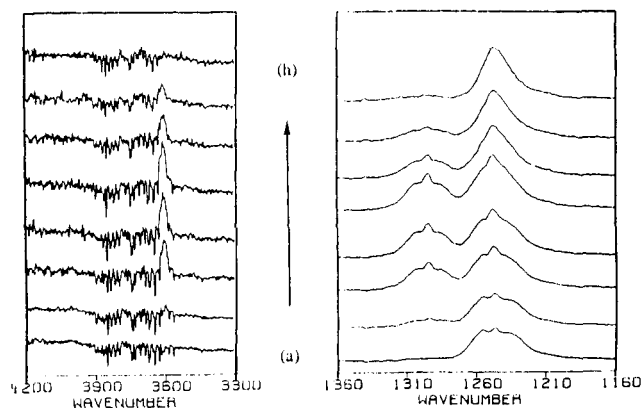
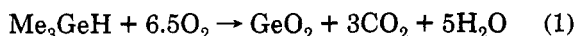


**Figure 6.** Spectra illustrating the growth and decay of bands due to the intermediate formed during the reaction of  $\text{Me}_3\text{GeH}$  and  $\text{O}_2$ . Labels are the same as in Figure 1.

20–30° higher for the initial onset of reaction than for experiments carried out in a preconditioned cell. Experiments carried out in the presence of varying amounts of ground Pyrex indicate a significant surface sensitivity on the second-order rate constants (Table 4). In each case the infrared cell was carefully conditioned both prior to and after each addition of ground glass in order to eliminate the possibility of a conditioning effect.

### Discussion

Even in the presence of a large excess of oxygen, over the temperature range 453–533 K the oxidation of trimethylgermane does not undergo exhaustive oxidation according to



Rather, under these conditions the Ge–C bond appears to be inert and  $\text{Me}_3\text{GeH}/\text{O}_2$  mixtures react via Ge–H bond fission, giving hexamethyldigermoxane and water:



The process is second order with respect to loss of  $\text{Me}_3\text{GeH}$

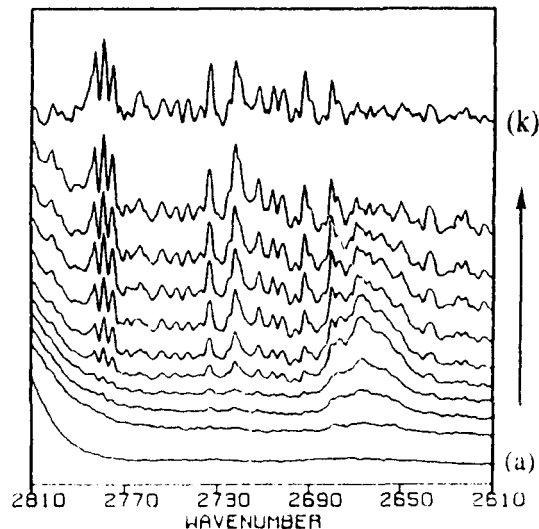


**Figure 7.** Spectra showing the  $\nu(\text{O}-\text{D})$  band of the reaction intermediate and the formation of  $\text{D}_2\text{O}$  during the decomposition of a  $\text{Me}_3\text{GeD}/\text{O}_2$  mixture at 493 K at (elapsed time after the start of the experiment in seconds) 0 (b), 330 (c), 570 (d), 1295 (e), 2260 (f), 2500 (g), 2980 (h), 3704 (i), and 6120 s (j). The spectrum of the initial reaction mixture at ambient temperature is shown in (a), and that of  $\text{D}_2\text{O}$  also at ambient temperature is shown in (k).

$\text{GeH}$  but zero order with respect to oxygen. Zero-order kinetics are strongly suggestive of the participation of an interface-mediated process, which is corroborated by the rate enhancement observed on increasing the available surface area by the addition of ground glass to the reaction cell. In the absence of oxygen, the thermolysis of  $\text{Me}_3\text{GeH}$  is a gas-phase process with little or no participation of the available surface in the reaction mechanism. In contrast, the oxidative thermolyses of both  $\text{Me}_4\text{Sn}$ <sup>15</sup> and  $\text{Me}_2\text{Sn}(\text{CH}=\text{CH}_2)_2$ <sup>16</sup> follow reaction pathways involving the formation of intermediate species formed by dissocia-

(15) Harrison, P. G.; Ashworth, A.; Clark, E. N.; McManus, J. *J. Chem. Soc., Faraday Trans.* 1990, 86, 4059.

(16) Harrison, P. G.; Clark, E. N. *J. Organomet. Chem.* 1992, 437, 145.

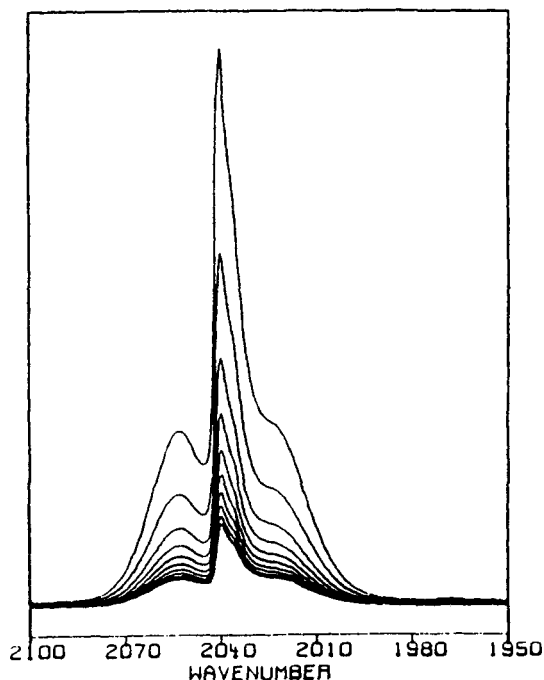


Figure 8. Spectra showing the decay of the  $\nu(\text{Ge-H})$  stretching envelope for the reaction of  $\text{Me}_3\text{GeH}$  and  $\text{O}_2$  at 513 K from time 0 to 1600 s.

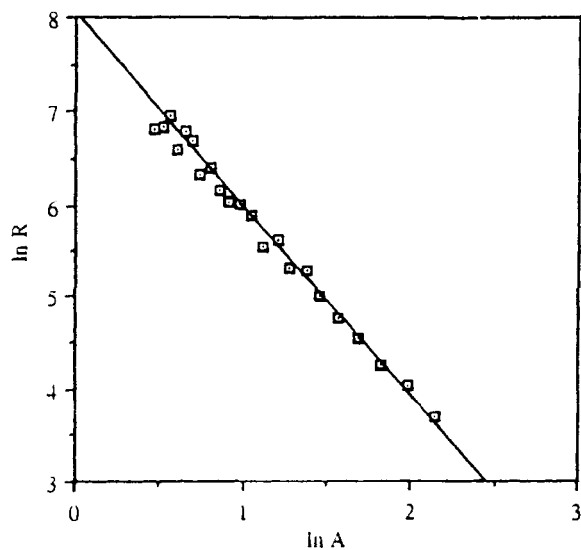
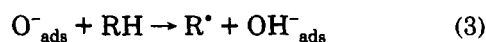


Figure 9. Van't Hoff plot for the reaction of  $\text{Me}_3\text{GeH}$  and  $\text{O}_2$  at 513 K.

tive chemisorption of the organostannane involving Sn-C bond fission at the solid-phase-gas-phase interface. The oxidation of hydrocarbons also usually involves the participation of a reactive surface where the reactive centers have been shown to be adsorbed paramagnetic oxygen ions of the types  $\text{O}^-$ ,  $\text{O}_2^-$ , and  $\text{O}_3^-$ . In all of these processes the initial step in the reaction sequence involves the abstraction of a hydrogen by a surface-adsorbed oxygen species:



Direct reaction between oxygen and hydrocarbon is less common.<sup>17,18</sup>

In the present case, the most probable initiation step is the abstraction of the hydrogen directly bonded to

(17) Russell, G. A. *J. Am. Chem. Soc.* 1956, 78, 1041.

(18) Bromberg, A.; Muszkat, K. A. *J. Am. Chem. Soc.* 1969, 91, 2860.

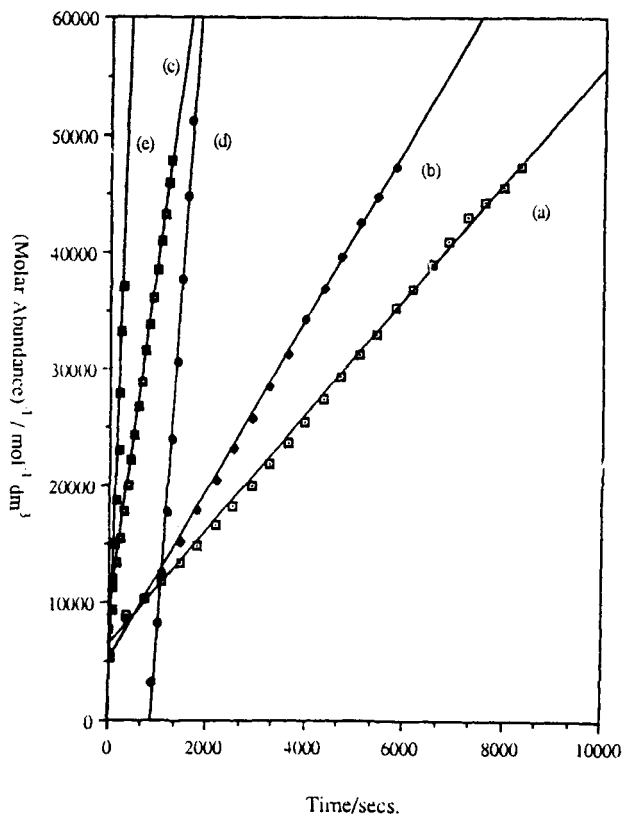


Figure 10. Second-order rate plots for the decomposition of 1:10 mole ratio mixtures of  $\text{Me}_3\text{GeH}$  and  $\text{O}_2$  at 493 K (a), 503 K (b), 513 K (c), 523 K (d), and 533 K (e). Straight lines indicate least-squares fits (minimum correlation coefficient 0.989).

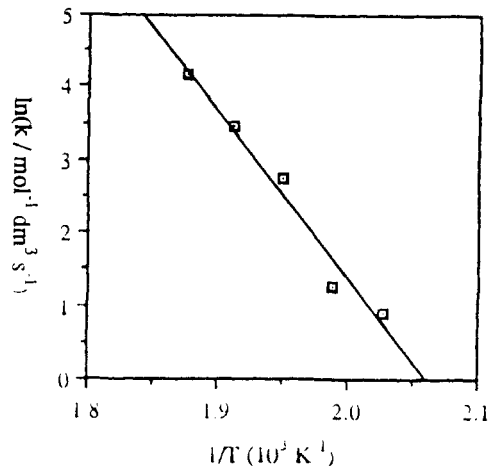


Figure 11. Arrhenius plot for the decomposition of 1:10 mole ratio mixtures of  $\text{Me}_3\text{GeH}$  and  $\text{O}_2$  in the temperature range 493–533 K. The straight line shows the least-squares fit (correlation coefficient 0.989).

Table 2. Second-Order Rate Constants for the Decomposition of 1:10 Trimethylgermane/ $\text{O}_2$  Mixtures

temp, K	rate constant $k$ , $\text{mol}^{-1} \text{dm}^3 \text{s}^{-1}$	temp, K	rate constant $k$ , $\text{mol}^{-1} \text{dm}^3 \text{s}^{-1}$
493	2.46	523	31.7
503	3.55	533	64.1
513	15.8		

germanium by a surface oxygen species (eq 4). The trimethylgermyl radical thus generated is then lost to the gas phase and reacts rapidly with oxygen, forming a (trimethylgermyl)peroxy radical (eq 5). This radical is converted by further H abstraction from  $\text{Me}_3\text{GeH}$  into

**Table 3. Second-Order Rate Constants for the Decomposition of Trimethylgermane/O<sub>2</sub> Mixtures of Varying Molar Ratio at 493 K**

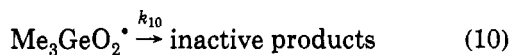
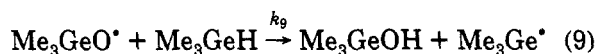
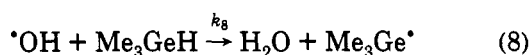
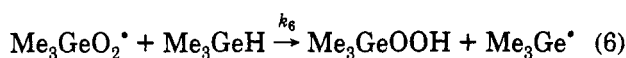
Me <sub>3</sub> GeH/ O <sub>2</sub> ratio	rate constant <i>k</i> , mol <sup>-1</sup> dm <sup>3</sup> s <sup>-1</sup>	Me <sub>3</sub> GeH/ O <sub>2</sub> ratio	rate constant <i>k</i> , mol <sup>-1</sup> dm <sup>3</sup> s <sup>-1</sup>
1:1	1.88	1:21	1.73
1:4	2.02	1:25	1.63
1:6	1.77	1:31	1.92
1:10	2.45		1.9(3) (mean)
1:15	2.11		

**Table 4. Second-Order Rate Constants Obtained for the Decomposition of 1:10 Trimethylgermane/O<sub>2</sub> Mixtures in the Presence of Ground Pyrex Glass at 493 K**

mass of ground glass added, g	rate constant <i>k</i> , mol <sup>-1</sup> dm <sup>3</sup> s <sup>-1</sup>	mass of ground glass added, g	rate constant <i>k</i> , mol <sup>-1</sup> dm <sup>3</sup> s <sup>-1</sup>
0	2.46	0.3	6.46
0.1	5.71	0.6	13.9

trimethylgermyl hydroperoxide (Me<sub>3</sub>GeOOH; eq 6), which undergoes O–O bond fission (eq 7). The (trimethylgermyl)oxyl and hydroxyl radicals thus produced propagate the reaction by H-abstraction from Me<sub>3</sub>GeH forming Me<sub>3</sub>GeOH and water (eqs 8 and 9). Hexamethyldigermoxane is subsequently produced by self-condensation of two Me<sub>3</sub>GeOH molecules (eq 11). This type of condensation is extremely facile, and attempts to isolate Me<sub>3</sub>GeOH have proved unsuccessful for this reason.<sup>19</sup> The reaction sequence is summarized in Scheme 1.

#### Scheme 1



Most of the steps in Scheme 1 have analogues in the mechanisms proposed for the autoxidation of hydrocarbons and the thermal decomposition of peroxides.<sup>17,18,20–24</sup> The initiation step (eq 4) is slow, so that at elevated

temperatures reaction 7 is the major source of free radicals. Implicit in this is that Me<sub>3</sub>GeOOH is unstable toward O–O bond homolysis. Although this particular compound has not been isolated, both triarylgermanium hydroperoxides, Ar<sub>3</sub>GeOOH, and bis(triarylgermanium) peroxides, Ar<sub>3</sub>GeOOGeAr<sub>3</sub>, decompose in solution *via* O–O bond fission.<sup>25</sup> Chain termination in autoxidation reactions is usually second order in peroxy radical concentration.<sup>26</sup> Both product analysis<sup>27</sup> and isotopic oxygen exchange<sup>28,29</sup> studies show that the head-to-head-coupled product RO<sub>4</sub>R is produced as either a transition state or an unstable intermediate. The germylperoxy radicals Re<sub>3</sub>GeOO• (R = Me, Ph), formed by reaction of the metal-centered radicals Me<sub>3</sub>M• with oxygen,<sup>30</sup> exist in equilibrium with the corresponding tetraoxide R<sub>3</sub>GeO<sub>4</sub>GeR<sub>3</sub> at low temperatures,<sup>31</sup> but at –50 °C the (triorganogermyl)peroxy radical decayed irreversibly with rates which were not a simple function of the radical concentration. However, at low radical concentration and high temperatures the decays of the peroxy radicals were first order. In contrast, the decays of the corresponding (triorganostannyl)peroxy radicals were second order in radical concentration and no evidence is apparent for a reversible equilibrium between the peroxy radical and the distannyl tetraoxide. Under the conditions used in the present case, the most probable radical chain termination process is unimolecular peroxy radical self-destruction at the cell wall rather than a gas-phase bimolecular coupling reaction.

Using the steady-state approximation, the reactions in Scheme 1 yield for the rate of loss of Me<sub>3</sub>GeH the expression

$$-\frac{d[\text{Me}_3\text{GeH}]}{dt} = 3 \left\{ \frac{k_4 k_6}{k_{10}} \right\} [\text{Me}_3\text{GeH}]^2 [\text{O}_{\text{ads}}] \quad (12)$$

predicting second-order dependence on Me<sub>3</sub>GeH but independence of gas-phase oxygen, in agreement with experimental observation. The rate expression also shows dependence on the concentration of active surface oxygen sites necessary for the initiation step, consistent with the observed effect of available surface area on the rate. From this expression it can be seen that three steps are important, the initiation step (eq 4), the termination step (eq 10), and the abstraction of the hydridic hydrogen bonded to Me<sub>3</sub>GeH by Me<sub>3</sub>GeOO• radicals (eq 6).

OM930758+

- (20) Bolland, J. L.; Gee, G. *Trans. Faraday Soc.* **1946**, *42*, 236.  
 (21) De la Mare, H. E.; Vaughan, W. E. *J. Chem. Educ.* **1957**, *34*, 64.  
 (22) Russell, G. A. *J. Chem. Educ.* **1959**, *36*, 111.  
 (23) Carlsson, D. J.; Robb, J. C. *Trans. Faraday Soc.* **1966**, *62*, 3403.  
 (24) Mayo, F. R. *Acc. Chem. Res.* **1968**, *1*, 193.  
 (25) Dannley, R. L.; Farrant, G. C. *J. Org. Chem.* **1969**, *34*, 2432.  
 (26) Sheldon, R. A.; Kochi, J. K. *Metal Catalyzed Oxidations of Organic Compounds*; Academic Press: New York, 1981; Chapter 2, pp 24–25.  
 (27) Blanchard, H. S. *J. Am. Chem. Soc.* **1959**, *81*, 4548.  
 (28) Bartlett, P. D.; Traylor, T. G. *J. Am. Chem. Soc.* **1963**, *85*, 2407.  
 (29) Bennet, J. E.; Howard, J. A. *J. Am. Chem. Soc.* **1973**, *95*, 4008.  
 (30) Bennet, J. E.; Howard, J. A. *J. Am. Chem. Soc.* **1972**, *94*, 8244.  
 (31) Howard, J. A.; Tait, J. C. *Can. J. Chem.* **1976**, *54*, 2669.

(19) Schafer, H. *Fresenius Z. Anal. Chem.* **1961**, *180*, 15.